Orbital
The electronic journal of chemistry

the electronic journal of chemistry

Full Paper | http://dx.doi.org/10.17807/orbital.v17i2.21048

Chemically Cross-linked Hydrogels Based on Cellulose Nanofibril for Oral Drug Delivery

Francielle Lopes [a], Luis Gustavo Pitlovanciv [b], André Luis Kerek [a], Jarem Raul Garcia [a], Barbara Celânia Fiorin [a], Michele Karoline Lima-Tenório [a], and Adriano Gonçalves Viana* [a]

Nanocellulose-based hydrogels have emerged as promising platforms for drug delivery in the gastrointestinal environment due to their biocompatible and biodegradable properties, aligning with the 3, 9, and 12 Sustainable Development Goals (SDG). In this study, we investigated the modification of cellulose nanofibrils (CNF) with glycidyl methacrylate and the subsequent synthesis of chemical hydrogels containing *N*′,*N*′-dimethylacrylamide (DMA), and sodium acrylate (NaAac). The structural and morphological characterization of the hydrogels was carried out using techniques such as FTIR (Fourier-transform infrared spectroscopy), ^{1}H NMR (proton Nuclear magnetic resonance), and SEM (scanning electron microscopy). The fluid absorption capacity and swelling kinetics were evaluated, as well as the contribution of swelling mechanisms to these processes. Among the formulations developed, H2 (50 mg of CNF, 50 mg of DMA, 50 mg of NaAac) was demonstrated to be responsive to changes in pH and ionic strength, which can potentially generate a material capable of acting as a carrier for controlled drug release systems in the gastrointestinal environment. This study suggests that modified CNF hydrogels have potential applications as a controlled release device in the gastrointestinal environment and contribute to achieving the SDG, offering a strategy to improve therapeutic efficacy, reduce side effects, and promote responsible consumption and production practices.

Graphical abstract

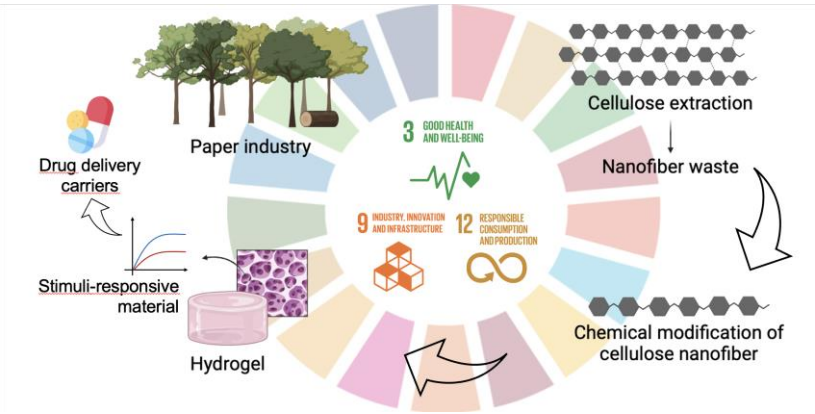

Keywords

Cellulose nanofiber
Drug delivery
Hydrogel
pH-responsive
Polysaccharide

Article history

Received 01 May 2204
Revised 02 Sep 2024
Accepted 17 Sep 2024
Available online 18 May 2025

Handling Editor: Sergio L. Lazaro

1. Introduction

The search for effective and sustainable drug delivery systems is a crucial challenge in the biomedical field, especially when considering the use of materials from natural and non-toxic origins. In this context, studies using hydrogels

[a] Department of Chemistry, State University of Ponta Grossa (UEPG), Av. General Carlos Cavalcanti – Uvaranas, zip code 84030-900 Ponta Grossa, Paraná, Brazil. [b] Department of Biology, State University of Ponta Grossa (UEPG), Av. General Carlos Cavalcanti – Uvaranas, zip code 84030-900 Ponta Grossa, Paraná, Brazil. *Corresponding author. E-mail: **adrianoviana@uepg.br**

as a drug delivery system have gained prominence for their ability to respond to external stimuli [1,2]. Hydrogels are formed by a three-dimensional polymeric network [3–6]. These materials can retain water or biological fluids and act as promising vehicles for controlled drug release [4,7]. For this aim, it is necessary the use of biocompatible and non-toxic materials, and for an eco-friendly approach, polysaccharides such as xanthan gum, chitosan, starch, agarose, and cellulose can be used for hydrogel synthesis [8–10].

Cellulose is the most abundant biopolymer in nature, can be obtained from plants or bacteria and its chemical structure consists of β-1,4-linked glucopyranose units [11–13]. It can be used in nanoscale sizes, such as nanocrystals and nanofibril, which present high mechanical strength [14,15]. These nanoscale materials have aroused interest due to their biocompatibility, biodegradability, and abundance of their raw material in nature [16–18]. The synthesis of hydrogels from cellulose nanofibril offers a promising approach for developing more sustainable and effective drug delivery systems [19–21]. Considering the global quest to achieve the 17 Sustainable Development Goals, the search for new drug delivery devices meets SDG 3: Good Health and Well-being, whose aims are to ensure healthy lives and promote well-being for all at all ages. We can also consider that research into new intelligent and responsive devices such as hydrogels meets the perspective of SDG 9: Industry, Innovation, and Infrastructure, bringing innovation to the pharmaceutical sector dealing with new biomaterials based on polysaccharides. Furthermore, the possibility of using waste from the paper industry as a source for the extraction of cellulose to produce new biomaterials, such as hydrogels, is in line with SDG 12: Sustainable Consumption and Production, which seeks to ensure sustainable standards of consumption and production, giving a new application to a product that would otherwise be discarded in the paper production cycle.

Therefore, in this work we investigated the modification of nanocellulose with glycidyl methacrylate and the subsequent synthesis of chemical hydrogels containing *N′,N′*-dimethylacrylamide and sodium acrylate as cross-linking agents, aiming a controlled drug release system. The morphology of the hydrogels and their water absorption capacity in response to the pH and ionic strength of the system were studied, in addition to the swelling kinetics. In this way, this study not only advances knowledge on the synthesis of cellulose nanofibril hydrogels, but also highlights their potential to drive progress towards the SDGs by promoting innovative and sustainable solutions in the biomedical field.

2. Results and Discussion

2.1 Chemical Modification of Cellulose Nanofibril

For the synthesis of chemical hydrogels based on cellulose nanofibril (CNF) via radical polymerization, a chemical modification was initially carried out to insert vinyl groups into the nanocellulose structure. The reaction was carried out under acidic conditions, where the epoxide ring-opening reaction resulted in two products: 3-methacryloyl-1-glyceryl ether of CNF, and 3-methacryloyl-2-glyceryl ether of CNF in higher concentration, and the mixture of these two products were called as CNF^{GMA} [22]. To confirm the chemical modification, Fourier Transform Infrared spectroscopy (FTIR) analysis was performed (Figure 1).

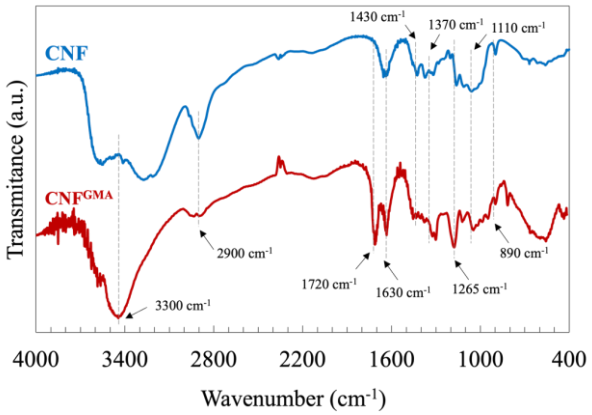

Fig. 1. FTIR spectra of CNF and CNF^{GMA}.

Characteristic bands, associated to chemical groups of nanocellulose, are observed on both spectra (CNF and CNF^{GMA}), showing the basic structure of cellulose was maintained after chemical modification. The band at 3300 cm^{-1}, refers to OH stretching; at 2900 cm^{-1}, is related to CH_2 asymmetric stretching. The band at 1630 cm^{-1}, indicates the C–C stretching band and combined with OH bending, from absorbed water. At 1430 cm^{-1}, there is a band which is attributed to CH_2 scissor vibration, from crystallized, and amorphous cellulose. The bands at 1370 cm^{-1}, 1265 cm^{-1}, and 1110 cm^{-1} are assigned to CH deformation, C-O-C bridge oxygen stretching, and C-O stretching, respectively. Finally, at 890 cm^{-1} there is a band which refers to the β-glycosidic bond between anhydroglucose units from cellulose. [23, 24].

The chemical modification of the polysaccharide with GMA can be proved by the bands at 1720 cm^{-1}, and 1630 cm^{-1}, which are attributed to stretching vibrations of carbonyl groups (vC=O), and vinyl groups (vC=C), respectively. In this way, in the spectrum of CNF^{GMA}, at 1630 cm^{-1}, there is an overlap of the C=C band of GMA, and the already existing band related to the C–C stretching combined with OH bending from absorbed water. The intensification of this band, as well as the appearance of a band at 1720 cm^{-1} in the CNF^{GMA} spectrum, confirms the chemical modification reaction. [22].

To obtain additional confirmation of the CNF^{GMA} structure, ^1H NMR was used to characterize the samples (Figure 2).

The ^1H NMR characterization for CNF in DMSO-D_6 is shown in Figure 2 as follows: 3.8-3.5 ppm for H2, H3, H4, H5 and H6; 4.4 ppm for C6-OH and 4.8-5.5 ppm for C3-OH, C2-OH and H1 [25]. For the GMA spectra, also in DMSO D_6 is 1.9 ppm for H14, 3.0-3.2 ppm for H12, 4.0 ppm for H11' and 4.5 for H11, 5.8 ppm for H7' and 6.1 ppm for H7. The addition of the vinyl groups in the nanocellulose structure can be observed by the chemical shifts at 6.1 and 5.8 ppm corresponding to H7 and H7', respectively, in the GMA and CNF^{GMA} spectra and structures (Figure 2) [26–29]. The signal at 1.9 ppm, corresponds to the hydrogens attached to the methyl carbon at GMA and CNF^{GMA} structures (H14, Figure 2) [26–28]. Considering that the chemical modification occurs via the opening of the epoxy ring, the signals in 2.8 and 2.6 ppm corresponding to H13 observed in the GMA spectrum and structure are not in the CNF^{GMA} [28,29]. The products obtained from 3-methacryloyl-1-glyceryl ether of CNF can be indirectly proven by the signals at 4.5 and 4.2 ppm that correspond to H18 and H20 in their structure [28]. The signals referring to 3-methacryloyl-2-glyceryl ether of CNF overlap the signals from CNF in the region of 3.5 - 4.5 ppm, the determination of the proportion between the products [22].

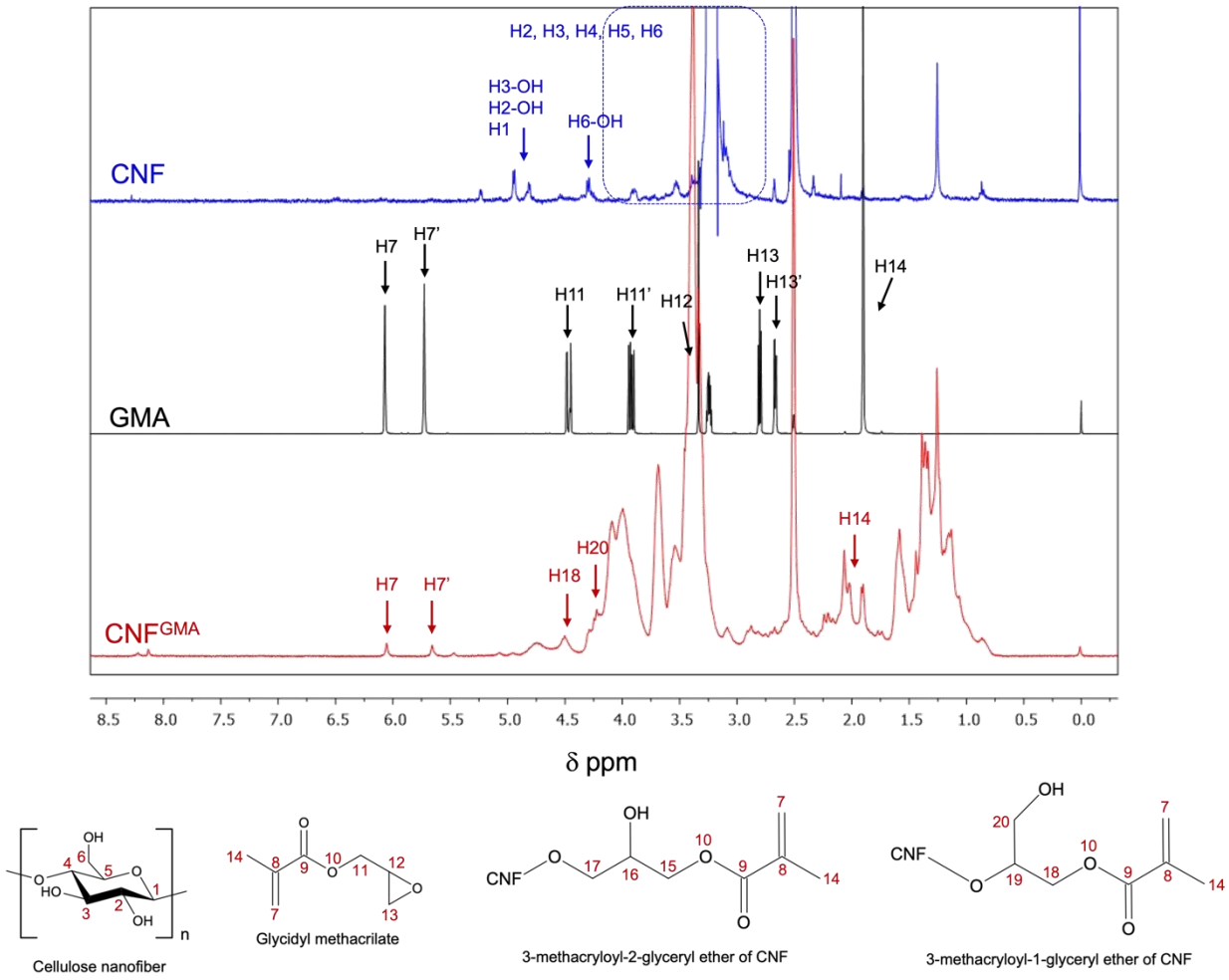

Fig. 2. ^{1}H NMR spectra of CNF, GMA, and CNF^{GMA}. and the structures of cellulose nanofibril, GMA, and both products of the nanocellulose chemical modification are shown along with their respective hydrogel assimilation.

2.2 Swelling in distilled water, ionic strength assays, and response to the pH of the environment

To study the hydrogel matrix ionic groups' behavior, swelling experiments were carried out in distilled water. These groups come from the sodium acrylate incorporated in one of the formulations. The same experiments allowed to understand the influence of the increased cross-linking density in the hydrogel matrix by increasing the concentration of the spacer agents in the formulations (*N*′,*N*′-dimethylacrylamide and sodium acrylate) in the swelling process. Figure 3A shows the results of a swelling degree in equilibrium (SW) for H1 e H2 hydrogels.

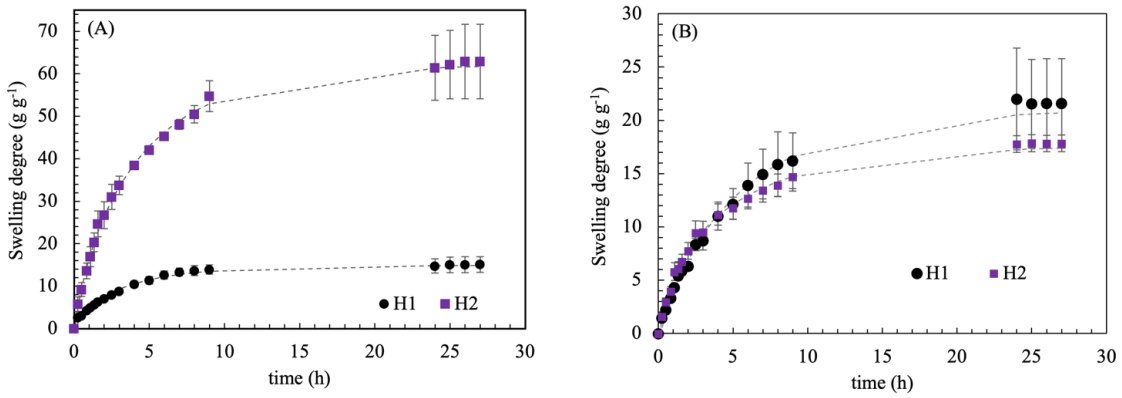

Fig. 3. Time-dependent swelling degree curves of H1, and H2 (A) at distilled water, and (B) at NaCl solution, both at 37 ºC.

Based on these experiments, the values of the SW were calculated using Equation 5, and the results are presented in Table 1. A noticeable contrast is observed between the SW values for H1 and H2. As expected, this difference could be related to the inclusion of sodium acrylate (NaAac) as a spacer agent in the H2 formulation, since in the H1 the only

spacer agent is *N',N'*-dimethylacrylamide (DMAam). The NaAac *p*Ka is 4.72 and it is negatively charged in aqueous solution. The insertion of the negative charges from carboxylate groups (COO^-) into this polymeric matrix triggers the increase of the electrostatic repulsion leading to greater separation among polymer chains and subsequently elevating the SW value at equilibrium [30,31]. On the other hand, H1 contains only DMAam, a neutral spacer agent that can reduce the process of the electrostatic repulsion in the hydrogel matrix, establishing hydrogen bonds between the functional groups, thus interfering with the swelling capacity and water retention since its contribution to swelling is only the presence of the hydrophilic groups in the structure [32]. This swelling behavior in distilled water can also be seen in hydrogels containing carboxylic acid and amine groups in their structure, since these are also found in the structure of the synthesized material [32, 33].

Table 1. Values of SW at equilibrium, the *k* and *d* constants for the Weibull fit, and *n* and *k* coefficients for the Power Law for the swelling assays in distilled water for H1 and H2 hydrogels.

		Weibull			Power Law Mechanism	
	SW	*k*	*d*	R^2	*n*	*k*
H1	15.12 ± 1.85[b]	0.448	0.770	0.991	0.75 ± 0.02	1.227 ± 0.111
H2	62.93 ± 8.77[a]	0.325	0.805	0.998	1.17 ± 0.03	1.827 ± 0.24

*Student's t test applied to samples H1 and H2 for SW values at distilled water solution with $p < 0.05$. Different letters in the column mean a significant difference between the values of SW.

To study the swelling kinetics, an adjustment using a Weibull function (Equation 1) was necessary to compare the equilibrium time for the two materials.

$$\frac{w_t}{w_{eq}} = (1 - e^{-kt^d}) \quad (1)$$

Once this adjustment has been made, two constants were calculated, denoted as *d* and *k*. The value of *k* is directly linked to the swelling rate for the material. In Table 01 we can notice that the *k* value for H1 in distilled water overcame the H2 value, indicating a higher swelling speed in H1. The average time taken by H1 to reach the equilibrium swelling was 11 hours, whereas it took 13.5 hours for H2. Although H2 took longer to reach the equilibrium, the difference between SW values can suggest that the ionic charge in the hydrogel matrix could contribute to the swelling process, since a difference in mass close to 75% was observed, comparing the SW values between the hydrogels, at the same time intervals.

To study the mechanism of water transport in H1 e H2 the Power Law equation (2) was applied [34]:

$$\frac{w_t}{w_{eq}} = kt^n \quad (2)$$

where *k* is the constant related to the kinetic behavior and the hydrogel matrix, and *n* is the diffusion coefficient that determines the swelling mechanism. Considering that both hydrogels were synthesized in a cylindrical shape, $n \leq 0.45$ refers to Fick's diffusion, $0.45 < n < 0.89$ corresponds to anomalous transport, and $n > 0.89$ refers to supercase II transport. As shown in Table 1, the value of *n* determined for H1 refers to anomalous transport, where both Fick diffusion and macromolecular relaxation contribute to the swelling mechanism. For H2, the *n* value refers to the supercase II transport mechanism, where the contribution of Fick's diffusion, macromolecular relaxation, and the erosion of polymer chains is observed. Thus, the main difference between the two hydrogels is the erosion in H2. In this hydrogel, the high SW value at equilibrium, which corresponds to 72 times the initial weight, can collapse the polymeric matrix, since the material cannot support the excess fluid.

The same analyses were carried out in NaCl solution aiming the study the hydrogel behavior in response to electrolytes in solution, simulating the ionic strength of the intestinal system. The swelling profile for H1 and H2 is shown in Figure 3B. For these tests, Weibull fit was also performed, and the water transport mechanism was studied using the Power Law equation. The results are presented in Table 2.

Table 2. Values of SW at equilibrium, the *k* and *d* constants for the Weibull fit, and *n* and *k* coefficients for the Power Law for the swelling assays in NaCl solution for H1 and H2 hydrogels.

	Weibull				Power Law Mechanism	
	SW	*k*	*d*	R^2	*n*	*k*
H1	21.59 ± 4.19[a]	0.243	0.859	0.993	0.79 ± 0.05	1.842 ± 0.142
H2	17.84 ± 0.79[a]	0.387	0.705	0.995	0.84 ± 0.04	1.489 ± 0.029

*Student's t test applied to samples H1 and H2 for SW values at NaCl solution with $p < 0.05$. Equal letters in the column mean that there is no significant difference between the values of SW.

Based on these experiments, the values of the SW on equilibrium for H1 e H2 were statistically equal, as we can see in Table 2, and the average time to reach the equilibrium was 19 hours for H1 and 18 hours for H2. The value of *n* determined for both hydrogels refers to an anomalous transport mechanism, since they were between 0.45 and 0.89, indicating the presence of both Fick's diffusion and macromolecular relaxation in the water transport process. When we compare these results with those obtained from the swelling in distilled water, no significant difference is observed between the SW values at equilibrium for H1, which suggests that the ionic strength of the medium does not affect the swelling process in this hydrogel. However, for H2, a 3.5x decrease in the SW value is observed. This result may be related to the neutralization of the carboxylate groups existing in the hydrogel matrix by sodium ions in solution, which allows the formation of hydrogen bonds between the polymer chains, resulting in a reduction in their swelling capacity [35]. Thus, in this environment, the SW value for H2 approaches the value obtained for H1, whose matrix is naturally neutral.

2.3 pH-responsivity assays

For swelling tests in a simulated gastrointestinal system, the ability to swell in the gastric system and intestinal system was evaluated separately. The SW values and swelling profile for the two formulations are shown in Figure 4. These tests allow evaluation of the material's ability to act as a drug carrier in a localized or controlled manner in simulated gastrointestinal fluid (SGIF).

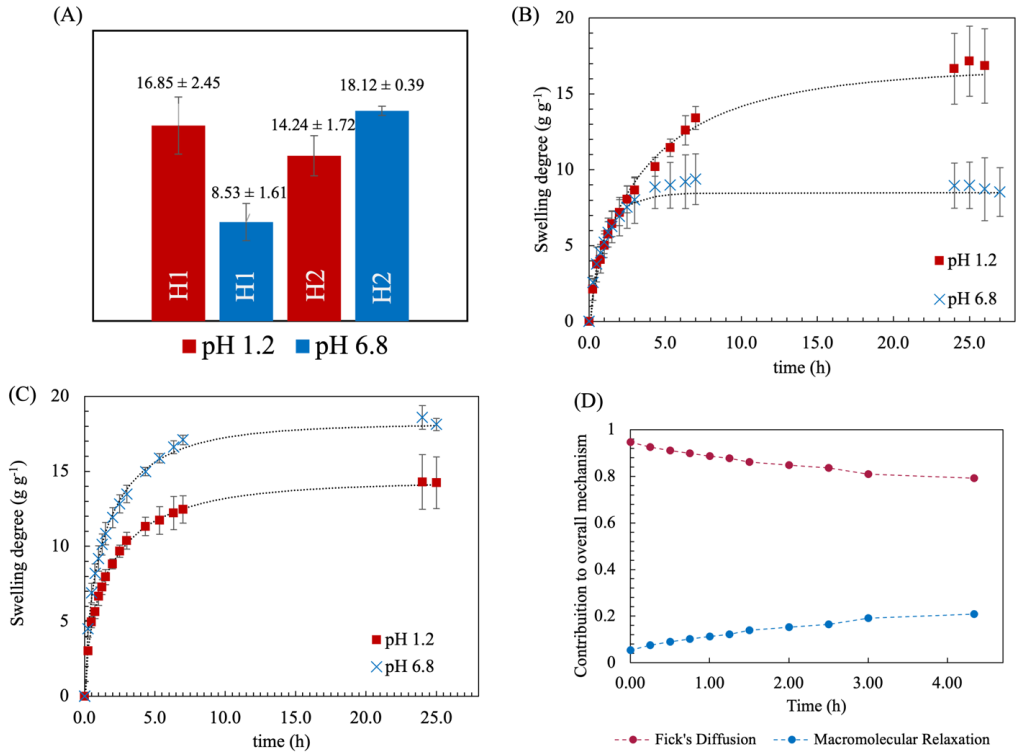

Fig. 4. (A) Values of SW at equilibrium for H1 and H2 in the SGF and SIF systems; Swelling profile of (B) H1 and (C) H2 in SGIF and (D) Fick's diffusion and macromolecular relaxation contributions to overall mechanism for H1 in SGF.

Both hydrogels showed significant differences between SW values after swelling tests in simulated gastric and intestinal fluid, as shown in Figure 4A. The H1 showed a higher SW value in an acidic environment (Figures 4A and 4B), indicating that this hydrogel would be a potential device for drug release in the stomach. However, we can observe that, at the initial times of the essay, H1 showed a very similar swelling profile at both analyzed pHs, which could result in a non-selective release of the drug. However, the H2 hydrogel showed a higher SW value at pH 6.8 (Figures 4A and 4C). This result may be related to the fact that at pH 1.2 the carboxylate groups of the polymeric matrix are protonated (COOH), which would help to establish intrachain hydrogen bonds, reducing the ability of the material to swell. On the other hand, at pH 6.8 the carboxylate groups are negatively charged (COO^-), causing repulsion between the polymer chains and making the swelling process easier [36]. To analyze the water transport mechanism, the Power Law model was used, and the values of the coefficients *n* and *k* are shown in Table 3.

Table 3. Values of SW at equilibrium. The coefficient *n* and the constant *k* of the Power Law equation were determined from the swelling tests for the hydrogels H1 and H2 at SGIF.

	SGF (pH 1.2)			SIF (pH 6.8)		
	SW	*n*	*k*	SW	*n*	*k*
H1	16.85 ± 2.45[a]	0.44 ± 0.07	1.090 ± 0.229	8.53 ± 1.61[b]	0.39 ± 0.12	0.421 ± 0.097
H2	14.24 ± 1.72[b]	0.41 ± 0.03	0.706 ± 0.137	18.12 ± 0.39[a]	0.39 ± 0.03	0.649 ± 0.045

*Student's t test applied to samples H1 and H2 for SW values at pH 1.2 and 6.8 solution with $p < 0.05$. Different letters in the lines mean that there is a significant difference in SW values at pH 1.2 and 6.8 for the same hydrogel.

As we can observe in the swelling assays at SGF, the *n* values of H1 showed a water transport mechanism between Fick's diffusion and anomalous transport while H2 showed a Fick's diffusion transport mechanism. To analyze the contribution of each mechanism to the overall water transport in H1 (Fick's diffusion and macromolecular relaxation) in the initial interval of the swelling process, the Peppas-Sahlin model [37] was applied and its equation (3) is described as follows:

$$\frac{w_t}{w_{eq}} = k_d t^{0,5} + k_r t \quad (3)$$

where k_d is the diffusion constant and k_r is the macromolecular relaxation constant. The value of k_r found was 0.027 and for k_d was 0.238 with a correlation coefficient of 0.935. With the values of both constants, it is possible to analyze the general contribution of each mechanism in the anomalous transport mechanism in the initial interval of the swelling process in SGF. The Fick's diffusion fraction was

determined using equation 4 and the macromolecular relaxation was determined with R = 1 – F.

$$F = \frac{1}{1+\frac{k_r}{k_d}t^{0.5}} \quad (4)$$

The result of the contribution of each mechanism to the overall water transport mechanism is shown in Figure 5D. At the initial time of the assay, the swelling process only follows the Fick diffusion mechanism. After 4 hours of experiment, however, a 20% contribution from the macromolecular relaxation mechanism in the swelling process was observed, indicating that the water transport mechanism is an anomalous transport. In SIF, both hydrogels showed a Fick's diffusion mechanism, despite a significant difference between the SW value between H1 and H2. This result showed that, in H1, the swelling mechanism changes with the change in the pH of the medium, but there is no inversion in the transport mechanism when it comes to the H2 formulation hydrogel. Despite maintaining the same swelling mechanism, in H2 there is a significant change in the swelling profile at the initial times in SGF and SIF, which would result in a localized release of the model drug.

Hydrogels with pH-responsive behaviors based on cellulose and its derivatives for the controlled release of drugs using different anionic spacer agents have been previously reported in the literature [38–40]. Materials containing acrylic acid as a spacer agent presented a profile similar to H2 swelling tests, in which a greater release of drugs in SIF can be observed [41–43]. Hydrogels cross-linked with DMAam and an anionic spacer also showed similar behaviors, with greater SW or drug release in the intestinal environment [44].

After reaching equilibrium at SIF, the internal morphology of CNF, H1, and H2 was observed and is shown in Figure 5. It is possible to observe that both H1 and H2 have a porous structure, resulting from the cross-links between the spacer agents and the nanocellulose chains. It is known that the porous structure of hydrogels is responsible for allowing the entry of fluids, which promotes the distension of the chains and the swelling of the material [45]. Furthermore, pores act as efficient sites for drug delivery when used as drug delivery devices. The greater number of pores observed in the H2 formulation hydrogel at pH 6.8 results in the highest SW value when compared to the result obtained for H1, which facilitates the entry of the fluid and consequent release of the drug in this formulation [46].

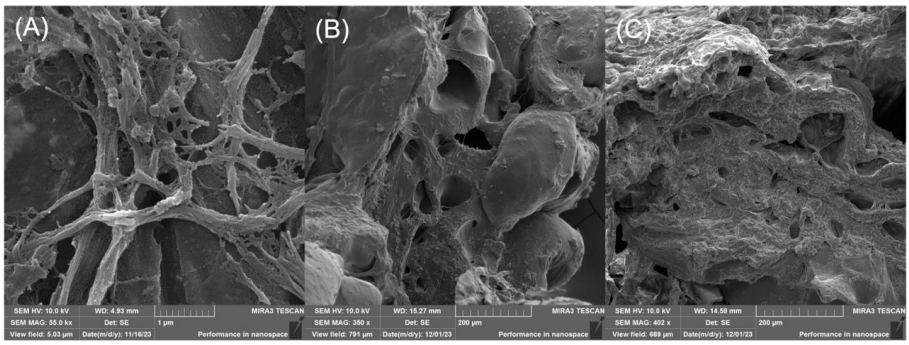

Fig. 5. SEM images for CNF (A), H1 (B) and H2 (C) after swelling at pH 6.8.

As a result of all the experiments, considering that H1 did not show a significant difference in the swelling process in the SGIF tests over the first 3 hours of the experiment, we understand that this material would not be suitable for application as a drug carrier, since its behavior in the gastric and intestinal systems are similar. The H2 swelling profile showed responsive behavior to pH variation, making it a potential vehicle for future studies in drug delivery. It can be explained by the swelling profile influence in the speed with which the drug would be released into the intestinal environment or at least prevent its release in the stomach. In this context, a technological application for cellulose nanofibril waste was found to meet the need to create materials that align with the needs of industrial innovation (SDG 9) and population health and well-being (SDG 3), aiming to achieve development using SDG 12 with the synthesis of materials based on consumption and sustainable production from industrial waste and cellulose recycling.

3. Material and Methods

3.1 Material

Monobasic potassium phosphate and sodium hydroxide (NaOH) were obtained from Dinâmica (Brazil). Glacial acetic acid and absolute ethanol were purchased from Perquim (Brazil), hydrochloric acid 37% from Reatech (Brazil), and acetone and sodium chloride from Neon (Brazil). *N*′,*N*′-dimethylacrylamide 99% (DMAam), glycidyl methacrylate 97% (GMA), sodium persulfate >98%, acrylic acid (AAc) was purchased from Sigma-Aldrich. Cellulose nanofibril (CNF) was obtained from the National Service of Industrial Learning (SENAI - Telêmaco Borba, Paraná, Brazil).

3.2 Cellulose nanofibril chemical modification

For the synthesis of chemical hydrogels, the cellulose nanofibril structure was previously modified with vinyl group addition [22]. For this reaction, 40 g of CNF suspension (0.028 g/g) were added to 100 mL of distilled water under stirring at a temperature of 60 ºC, and the pH of the solution was adjusted to approximately 4.0, with glacial acetic acid. Then, 0.044 mol of glycidyl methacrylate (GMA) was added and the solution was left under stirring for 24 h. The modified cellulose nanofibril (CNF^{GMA}) was precipitated with 300 mL of ethanol, filtered, and dried at room temperature. To confirm the chemical modification of CNF, FTIR spectra were recorded (Shimadzu/IRPrestige-21 spectrometer). The samples were analyzed as dry powders prepared into KBr pellets, with a total of 64 scans per spectrum to achieve a resolution of 2 cm^{-1}, covering the range from 4000 to 400 cm^{-1}. The samples were also characterized by Nuclear Magnetic Resonance Spectroscopy. The ^1H spectra were acquired using a Bruker

400 MHz spectrometer (model AVANCE III), operating at frequencies of 400.0 MHz for ^{1}H nucleus. For the acquisition of spectra, 20 mg of powdered samples were dissolved in 0.6 mL of $DMSO_d6$ containing 0.05% of 3-(trimethylsilyl)propionic-2,2,3,3$_d$4 acid sodium salt (TMS) as an internal standard.

3.3 Sodium acrylate synthesis

Sodium acrylate (NaAac) was used as an anionic spacer agent on the hydrogel synthesis. For its preparation, 0.71 mol of acrylic acid was solubilized in acetone under mild stirring. Then, 0.71 mol of NaOH was slowly added to the solution, forming a white precipitate (NaAac). The salt was filtered and left to dry in an oven at 40 ºC.

3.4 Synthesis of CNF^{GMA} based hydrogels

The radical polymerization method was used for the synthesis of chemical hydrogels. [45]. Previously, for the gelation reaction, 50.0 mg of CNF^{GMA} and different amounts of *N',N'*-dimethylacrylamide and NaAac (Table 4) were added in distilled water reaching the final volume of 5.0 mL. The mixture was kept under stirring and heated to 60 ºC and 17.0 mg (6.2 x 10^{-5} mol) of potassium persulfate was added. After the initiator was solubilized in the solution, the heating and stirring were interrupted and the hydrogel was formed. The hydrogels were then fractured, dialyzed against distilled water, dried in an oven at 60 ºC, and then stored.

Table 4. Hydrogel formulations based on CNF^{GMA}, DMAam and NaAac.

Hydrogel	CNF^{GMA} (mg)	DMAam (mol)	NaAac (mol)
H1	50.0	5.3 x 10^{-3}	0
H2	50.0	4.8 x 10^{-3}	5.3 x 10^{-4}

3.5 Hydrogel morphology

The internal morphology of the synthesized hydrogels was analyzed using scanning electron microscopy (SEM/Tescan – Mira 3). After reaching swelling equilibrium at pH 6.8, the materials were frozen by immersion in liquid nitrogen and then lyophilized for 72 h to preserve the material's internal morphology. The samples were fractured and coated with a thin layer of gold and the images were obtained with an acceleration voltage of 15 kV and a current intensity of 106 mA.

3.6 Swelling measurements, ionic strength, and pH-responsivity analysis

The swelling measurements were made to simulate the hydrogel swelling at simulated gastrointestinal fluid [47]. For the saline solution that simulated the same ionic force as the gastric media, a sodium chloride solution of 10.85 g L^{-1} was prepared. The simulated fluids were prepared following the U.S. Pharmacopeia in the absence of enzymes. For this purpose, simulated gastric fluid (SGF) of pH 1.2 was prepared with a solution of 2.0 g L^{-1} of sodium chloride and 0.08 mol L^{-1} of hydrochloric acid, and the simulated intestinal fluid (SIF) of pH 6.8 was prepared with 0.62 g L^{-1} of sodium hydroxide and 6.80 g L^{-1} of monobasic potassium phosphate.

To obtain SW, a gravimetric assay was performed, where a dried hydrogel sample was submersed to the SGF or SIF solutions at a controlled temperature of 37 ºC. In specific time intervals, the hydrogels were withdrawn from the solution and then weighed after removing the solution from the surface. The swelling degree was obtained using equation 5, where w_t is hydrogel weight in time and w_0, the weight of the dried hydrogel. The assays were performed in triplicate.

$$SW = \frac{w_t - w_0}{w_t} \quad (5)$$

4. Conclusions

The CNF was modified with the vinyl group using GMA as the modifying reagent. This material exhibited potential for use as a precursor for hydrogels displaying pH-responsive behavior when synthesized with spacer agents DMAam and NaAac. Hydrogel H1 demonstrated a similar swelling pattern in distilled water and NaCl solution, indicating an anomalous transport mechanism for water. On the other hand, hydrogel H2 contains carboxylate groups that are in ionic form in distilled water, leading to increased SW values due to electrostatic repulsion within the polymeric matrix. In the NaCl solution, the SW value decreases as a result of ion presence. Regarding pH-responsive assays, only hydrogel H2 displayed encouraging results for gastrointestinal delivery by exhibiting greater release in intestinal media and higher SW values at pH 6.8.

Acknowledgments

The authors would like to thank Geraldo de Aguiar Coelho from SENAI/PR for the cellulose nanofibril supply, the multi-user lab (C-LabMu) from State University of Ponta Grossa (UEPG - Brazil) for providing equipment and carrying out analyses. Lopes, F. (88887.688572/2022-00) and Kerek, A. L (88887.650540/2021-00) would like to thank Coordenação de Aperfeiçoamento de Pessoal de Nível Superior (CAPES) for doctoral fellowships and Pitlovanciv, L. G. would like to thank Universidade Estadual de Ponta Grossa for the PIBITI (Programa Institucional de Bolsas de Iniciação em Desenvolvimento Tecnológico e Inovação) fellowship.

Author Contributions

Francielle Lopes: Conceptualization, Data Curation, Formal Analysis, Investigation, Methodology, Validation, Visualization, Writing – Original Draft. Luis Gustavo Pitlovanciv: Formal Analysis; André Luis Kerek: Formal Analysis, Investigation; Jarem Raul Garcia: Resources. Barbara Celânia Fiorin: Formal Analysis. Michele Karoline Lima-Tenório: Writing – Review & Editing. Adriano Gonçalves Viana: Visualization, Resources, Project Administration, Writing – Review & Editing, Supervision.

References and Notes

[1] Bora, A.; Sarmah, D.; Rather, M. A.; Mandal, M.; Karak, N. *Int. J. Biol. Macromol.* **2024**, *256*, 128253. [Crossref]

[2] Günter, E. A.; Melekhin, A. K.; Belozerov, V. S.; Martinson, E. A.; Litvinets, S. G. *Int. J. Biol. Macromol.* **2024**, *258*, 128935. [Crossref]

[3] Ansar, R.; Saqib, S.; Mukhtar, A.; Niazi, M. B. K.; Shahid, M.; Jahan, Z.; Kakar, S. J.; Uzair, B.; Mubashir, M.; Ullah, S.; Khoo, K. S.; Lim, H. R.; Show, P. L. *Chemosphere* **2022**, *287*, 131956. [Crossref]

[4] Noor, F.; Mahmood, A.; Zafar, N.; Sarfraz, R. M.; Rehman, U.; Ijaz, H.; Hussain, Z.; Ahmed, I. A.; Imam, M.

T.; Al Abdulmonem, W.; Yadav, K. K.; Benguerba, Y. *J. Drug Deliv. Sci. Technol.* **2023**, *88*, 104924. [Crossref]

[5] Rabeh, M. E.; Vora, L. K.; Moore, J. V.; Bayan, M. F.; McCoy, C. P.; Wylie, M. P. *Biomaterials Advances* **2024**, *157*, 213735. [Crossref]

[6] Raeisi, A.; Farjadian, F. *Front Chem* **2024**, *12*. [Crossref]

[7] Medha; Sethi, S. *Mater. Today Commun.* **2024**, *38*, 108029. [Crossref]

[8] Zong, S.; Wen, H.; Lv, H.; Li, T.; Tang, R.; Liu, L.; Jiang, J.; Wang, S.; Duan, J. *Carbohydr. Polym.* **2022**, *278*, 118943. [Crossref]

[9] Ning, L.; You, C.; Zhang, Y.; Li, X.; Wang, F. *Composites Communications* **2021**, *26*, 100739. [Crossref]

[10] Irfan, J.; Ali, A.; Hussain, M. A.; Haseeb, M. T.; Naeem-ul-Hassan, M.; Hussain, S. Z. *RSC Adv* **2024**, *14,* 8018. [Crossref]

[11] Müller, A.; Wesarg, F.; Hessler, N.; Müller, F. A.; Kralisch, D.; Fischer, D. *Carbohydr. Polym.* **2014**, *106*, 410. [Crossref]

[12] Wei Wei Tay, K.; Fun Chin, S.; Wasli, M. E.; Musa, Z. *Pertanika J. Sci. Technol.* **2023**, *31*, 2805. [Crossref]

[13] Mojahedi, M.; Zargar Kharazi, A.; Poorazizi, E. *Polym. Eng. Sci.* **2024**. [Crossref]

[14] Ning, L.; You, C.; Zhang, Y.; Li, X.; Wang, F. *Life Sci.* **2020**, *241*, 117137. [Crossref]

[15] Ning, L.; You, C.; Zhang, Y.; Li, X.; Wang, F. *Composites Communications* **2021**, *26*, 100739. [Crossref]

[16] Liu, Y.; Fan, Q.; Huo, Y.; Li, M.; Liu, H.; Li, B. *Cellulose* **2021**, *28*, 6953. [Crossref]

[17] Liu, Y.; Huo, Y.; Li, M.; Qin, C.; Liu, H. *Cellulose* **2022**, *29*, 379. [Crossref]

[18] Misaka, M.; Teshima, H.; Hirokawa, S.; Li, Q.-Y.; Takahashi, K. *Surfaces and Interfaces* **2024**, *46*, 103923. [Crossref]

[19] Verma, A.; Sharma, B.; Kalia, S.; Alsanie, W. F.; Thakur, S.; Thakur, V. K. *Int. J. Biol. Macromol.* **2023**, *228*, 773. [Crossref]

[20] Islam, Md. S.; Alam, M. N.; van de Ven, Theo. G. M. *Cellulose* **2020**, *27*, 7637. [Crossref]

[21] Khamrai, M.; Banerjee, S. L.; Paul, S.; Samanta, S.; Kundu, P. P. *Int. J. Biol. Macromol.* **2019**, *122*, 940. [Crossref]

[22] Reis, A. V.; Fajardo, A. R.; Schuquel, I. T. A.; Guilherme, M. R.; Vidotti, G. J.; Rubira, A. F.; Muniz, E. C. *J. Org. Chem.* **2009**, *74*, 3750. [Crossref]

[23] Ning, L.; You, C.; Zhang, Y.; Li, X.; Wang, F. *Composites Communications* **2021**, *26*, 100739. [Crossref]

[24] Kotov, N.; Larsson, P. A.; Jain, K.; Abitbol, T.; Cernescu, A.; Wågberg, L.; Johnson, C. M. *Carbohydr. Polym.* **2023**, *302*, 120320. [Crossref]

[25] Jiang, F.; Dallas, Jerry. L.; Ahn, B. K.; Hsieh, Y.-L. *Carbohydr. Polym.* **2014**, *110*, 360. [Crossref]

[26] Wu, D.; Li, J.; Wang, C.; Su, Z.; Su, H.; Chen, Y.; Yu, B. *Mater. Today Bio.* **2024**, *25*, 100962. [Crossref]

[27] Li, T.; Liu, J.; Bin, F.-C.; Duan, Q.; Wu, X.-Y.; Dong, X.-Z.; Zheng, M.-L. *ACS Appl. Bio. Mater.* **2024**, *7*, 2594. [Crossref]

[28] Lima-Tenório, M. K.; Tenório-Neto, E. T.; Guilherme, M. R.; Garcia, F. P.; Nakamura, C. V.; Pineda, E. A. G.; Rubira, A. F. *Chem. Eng. J.* **2015**, *259*, 620. [Crossref]

[29] Tenório-Neto, E. T.; Guilherme, M. R.; Lima-Tenório, M. K.; Scariot, D. B.; Nakamura, C. V.; Rubira, A. F.; Kunita, M. H. *Colloid Polym. Sci.* **2015**, *293*, 3611 [Crossref]

[30] Jiang, Z.; Shi, X.; Qiao, F.; Sun, J.; Hu, Q. *Biomacromolecules* **2022**, *23*, 5239. [Crossref]

[31] Bukhari, S. M. H.; Khan, S.; Rehanullah, M.; Ranjha, N. M. *Int. J. Polym. Sci.* **2015**, *2015*, 1. [Crossref]

[32] Valencia-May, E. G.; Rivera, E.; Novelo-Peralta, O.; Burillo, G. *Radiation Physics and Chemistry* **2022**, *194*, 109975. [Crossref]

[33] Hua, B. Y.; Wei, H. L.; Hu, C. W.; Zhang, Y. Q.; Yang, S.; Wang, G.; Shen, Y. M.; Li, J. J. *Int. J. Environ. Sci. Technol.* **2024**, *21*, 227. [Crossref]

[34] Peppas, N. A.; Colombo, P. *J. Controlled Release* **1997**, *45*, 35. [Crossref]

[35] Sun, W.; Wang, J.; He, M. *Carbohydr. Polym.* **2023**, *303*, 120446. [Crossref]

[36] Yang, X.; Li, Z.; Liu, H.; Ma, L.; Huang, X.; Cai, Z.; Xu, X.; Shang, S.; Song, Z. *Int. J. Biol. Macromol.* **2020**, *143*, 190. [Crossref]

[37] Peppas, N. A.; Sahlin, J. J. *Int. J. Pharm.* **1989**, *57*, 169. [Crossref]

[38] Chen, X. Y.; Butt, A. M.; Mohd Amin, M. C. I. *J. Controlled Release* **2019**, *311–312*, 50. [Crossref]

[39] Batool, N.; Sarfraz, R. M.; Mahmood, A.; Zaman, M.; Zafar, N.; Salawi, A.; Almoshari, Y.; Alshamrani, M. *Gels* **2022**, *8*, 190. [Crossref]

[40] Ashames, A.; Pervaiz, F.; Al-Tabakha, M.; Khalid, K.; Hassan, N.; Shoukat, H.; Buabeid, M.; Murtaza, G. *J. Saudi Chem. Soc.* **2022**, *26*, 101541. [Crossref]

[41] Pinto e Souza, I. E.; Barrioni, B. R.; Costa, M. C. P.; Miriceia, N. M. L.; Sachs, D.; Ribeiro, G. C.; Soares, D. C. F.; Pereira, M. M.; Nunes, E. H. M. *Mater. Today Commun.* **2024**, *38*, 107981. [Crossref]

[42] Suhail, M.; Chiu, I.-H.; Liu, J.-Y.; Ullah, H.; Lin, I.-L.; Minhas, M. U.; Tsai, M.-J.; Wu, P.-C. *Curr. Pharm. Des.* **2023**, *29*, 2489. [Crossref]

[43] Farid-ul-Haq, M.; Hussain, M. A.; Ali, A.; Haseeb, M. T.; Muhammad, G.; Tabassum, T.; Ashraf, M. U.; Tulain, U. R.; Erum, A. *J. Drug Deliv. Sci. Technol.* **2024**, *93*, 105468. [Crossref]

[44] Aslam, A.; Umer Ashraf, M.; Barkat, K.; Mahmood, A.; Muhammad Sarfraz, R.; Malatani, R. T.; Gad, H. A. *Int. J. Pharm.* **2023**, *644*, 123305. [Crossref]

[45] Reis, A. C.; dos Santos, L. V.; Santos, K. R.; Lima-Tenório, M. K.; Paludo, K. S.; Maurício, M. R.; Rubira, A. F.; Viana, A. G.; Tenório-Neto, E. T. *Int. J. Pharm.* **2022**, *617*, 121626. [Crossref]

[46] Simayi, R.; Zhang, X.; Sawut, A.; Zhu, Z.; Wu, T.; Jiang, M. *ChemistrySelect* **2024**, *9*. [Crossref]

[47] Corona-Escalera, A. F.; Tinajero-Díaz, E.; García-Reyes, R. A.; Luna-Bárcenas, G.; Seyfoddin, A.; Padilla-de la Rosa, J. D.; González-Ávila, M.; García-Carvajal, Z. Y. *Pharmaceutics* **2022**, *14*, 2759. [Crossref]

How to cite this article

Lopes, F.; Pitlovanciv, L. G.; Kerek, A. L.; Garcia, J. R.; Fiorin, B. C.; Tenório, M. L. L.; Viana A. G. *Orbital: Electronic J. Chem*. **2025**, *17*, 226. DOI: http://dx.doi.org/10.17807/orbital.v17i2.21048